J|A|C|S
ARTICLES
Published on Web 05/20/2006

How Nitrogenase Shakes − Initial Information about P−Cluster and FeMo-cofactor Normal Modes from Nuclear Resonance Vibrational Spectroscopy (NRVS)

Yuming Xiao,[†] Karl Fisher,[§] Matt C. Smith,[†] William E. Newton,*[,§] David A. Case,*[,||] Simon J. George,[‡] Hongxin Wang,[†,‡] Wolfgang Sturhahn,[⊥] Ercan E. Alp,[⊥] Jiyong Zhao,[⊥] Yoshitaka Yoda,[#] and Stephen P. Cramer*[,†,‡]

Contribution from the Department of Applied Science, University of California, Davis, California 95616, Physical Biosciences Division, Lawrence Berkeley National Laboratory, Berkeley, California 94720, Department of Biochemistry, Virginia Tech, Blacksburg, Virginia 24061, Department of Molecular Biology, The Scripps Research Institute, La Jolla, California 92037, Advanced Photon Source, Argonne National Laboratory, Argonne, Illinois 60439, and JASRI, SPring-8, 1-1-1 Kouto, Sayo-cho, Sayo-gun, Hyogo 679-5198, Japan

Received January 26, 2006; E-mail: cramer@lbl.gov; wenewton@vt.edu; case@scripps.edu

Abstract: Nitrogenase catalyzes a reaction critical for life, the reduction of N_2 to $2NH_3$, yet we still know relatively little about its catalytic mechanism. We have used the synchrotron technique of ^{57}Fe nuclear resonance vibrational spectroscopy (NRVS) to study the dynamics of the Fe−S clusters in this enzyme. The catalytic site FeMo-cofactor exhibits a strong signal near 190 cm^{-1}, where conventional Fe−S clusters have weak NRVS. This intensity is ascribed to cluster breathing modes whose frequency is raised by an interstitial atom. A variety of Fe−S stretching modes are also observed between 250 and 400 cm^{-1}. This work is the first spectroscopic information about the vibrational modes of the intact nitrogenase FeMo-cofactor and P-cluster.

Introduction

Biological nitrogen fixation, involving reduction of dinitrogen to ammonia, is the key reaction in the nitrogen cycle and the ultimate source for most nitrogen in living systems.[1−3] In *Azotobacter vinelandii* (*Av*) the Mo-dependent nitrogenase (N_2ase) that accomplishes this reaction uses electrons from an Fe_4S_4 cluster in the ∼63 kDa Fe protein (*Av2*) in a MgATP-dependent reaction to reduce the ∼230 kDa $\alpha_2\beta_2$ MoFe protein (*Av1*). Within the latter, an Fe_8S_7 "P-cluster" supplies electrons to the active site $MoFe_7S_9$ "FeMo-cofactor", which is extractable into organic solvents as "FeMoco".[4]

A recent structure for *Av1* at 1.16 Å resolution[5] revealed electron density at the center of the trigonal prismatic cage of Fe atoms in the FeMo-cofactor and, hence, an overall $MoFe_7S_9X$ core cluster composition. The electron density is consistent with a light (C, N, or O) atom. Characterization of the interstitial atom is essential for understanding both the biosynthesis of the FeMo-cofactor and the mechanism of nitrogenase. Although ENDOR and ESEEM experiments have revealed several ^{14}N signals that are weakly coupled to the FeMo-cofactor spin, none of these exchange when the enzyme is turned over under $^{15}N_2$.[6] Furthermore, when *Azotobacter vinelandii* (*Av*) is grown on ^{15}N-urea, no ^{15}N ENDOR signals are observed from the extracted FeMo-cofactor.[7]

Numerous DFT calculations have been performed using X = C, N, or O, as well as with an empty central site.[8−16] These studies point toward N as the most likely interstitial atom (but do not exclude C or O); in some models X is inert, whereas, in

[†] University of California.
[‡] Lawrence Berkeley National Laboratory.
[§] Virginia Tech.
[||] The Scripps Research Institute.
[⊥] Argonne National Laboratory.
[#] JASRI.

(1) Igarashi, R. Y.; Seefeldt, L. C. *Crit. Rev. Biochem. Mol. Biol.* **2003**, *38*, 351−384.
(2) Rees, D. C.; Tezcan, F. A.; Haynes, C. A.; Walton, M. Y.; Andrade, S.; Einsle, O.; Howard, J. B. *Philos. Trans. R. Soc. London, Ser. A* **2005**, *363*, 971−984.
(3) Dos Santos, P. C.; Igarashi, R. Y.; Lee, H.-I.; Hoffman, B. M.; Seefeldt, L. C.; Dean, D. R. *Acc. Chem. Res.* **2005**, *38*, 208−214.
(4) Pickett, C. J.; Vincent, K. A.; Ibrahim, S. K.; Gormal, C. A.; Smith, B. E.; Best, S. P. *Chemistry* **2003**, *9*, 76−87.
(5) Einsle, O.; Tezcan, F. A.; Andrade, S. L. A.; Schmid, B.; Yoshida, M.; Howard, J. B.; Rees, D. C. *Science* **2002**, *297*, 1696−1700.
(6) Lee, H.-I.; Benton, P. M. C.; Laryukhin, M.; Igarashi, R. Y.; Dean, D. R.; Seefeldt, L. C.; Hoffman, B. M. *J. Am. Chem. Soc.* **2003**, *125*, 5604−5605.
(7) Yang, T.-C.; Maeser, N. K.; Laryukhin, M.; Lee, H.-I.; Dean, D. R.; Seefeldt, L. C.; Hoffman, B. M. *J. Am. Chem. Soc.* **2005**, *127*, 12804−12805.
(8) Dance, I. *Chem. Commun.* **2003**, 324−325.
(9) Hinnemann, B.; Nørskov, J. K. *J. Am. Chem. Soc.* **2003**, *125*, 1466−1467.
(10) Schimpl, J.; Petrilli, H. M.; Blochl, P. E. *J. Am. Chem. Soc.* **2003**, *125*, 15772−15778.
(11) Lovell, T.; Liu, T.; Case, D. A.; Noodleman, L. *J. Am. Chem. Soc.* **2003**, *125*, 8377−8383.
(12) Huniar, U.; Ahlrichs, R.; Coucouvanis, D. *J. Am. Chem. Soc.* **2004**, *126*, 2588−2601.
(13) Hinnemann, B.; Nørskov, J. K. *J. Am. Chem. Soc.* **2004**, *126*, 3920−3927.
(14) Dance, I. *J. Am. Chem. Soc.* **2004**, *126*, 11852−11863.
(15) Dance, I. *J. Am. Chem. Soc.* **2005**, *127*, 10925−10942.
(16) Kastner, J.; Blochl, P. E. *ChemPhysChem* **2005**, *6*, 1724−1726.

10.1021/ja0603655 CCC: $33.50

others, it is a product of the reaction mechanism. Clearly, the nature of X cannot be decided by theory alone, and new experimental approaches are required for the characterization of N_2ase and for determining the nature of atom X.

We report here the first information about vibrational modes of the Fe−S clusters in N_2ase, using the technique of nuclear resonance vibrational spectroscopy (NRVS).[17] In this experiment, a highly monochromatic X-ray beam is scanned through a nuclear (in this case ^{57}Fe) resonance. On the wings of the familiar "recoil-free" Mössbauer resonance are additional features that correspond to nuclear transitions combined with either excitation or de-excitation of vibrational modes. NRVS theory has been explained elsewhere;[17] key to the current study is that intensity of a normal mode is proportional to the fraction of kinetic energy derived from ^{57}Fe. From NRVS data, one can obtain an ^{57}Fe-specific partial vibrational density of states (PVDOS) that complements infrared and Raman spectra.

Experimental Section

Cell Growth and Purification of Nitrogenase Proteins. The *Av* wild-type strain was grown in the absence of a fixed-nitrogen source in a 24-L fermenter at 30 °C in a modified, liquid Burk medium.[18] All cultures contained 20 μM $^{57}FeCl_3$ and 10 μM Na_2MoO_4 and were grown to a final cell density of 250 Klett units recorded on a Klett−Summerson meter equipped with a number 54 filter. All manipulations of N_2ase proteins were performed anaerobically using either a Schlenk line or an anaerobic glovebox operating at less than 1 ppm O_2. After harvesting, cell extracts were prepared by diluting the whole cells with an equal amount of 50 mM Tris pH 8.0 prior to passage through a French pressure cell and centrifugation at 98 000 g for 90 min. N_2ase component proteins were separated by anaerobic Q-Sepharose anion-exchange column chromatography using a linear NaCl concentration gradient. *Av2* was purified to homogeneity by fractionation from a second Q-Sepharose column. *Av2* used in these experiments was obtained from a parallel growth that contained $^{56}FeCl_3$. *Av1* was further purified by Sephacryl S-200 gel filtration and phenyl-Sepharose hydrophobic-interaction chromatography.[19] The purified N_2ase proteins were concentrated individually using an Amicon microfiltration pressure concentrator before buffer exchange to 25 mM HEPES pH 7.5, 100 mM NaCl, 10 mM $MgCl_2$, and 2 mM $Na_2S_2O_4$ by dialysis at 4 °C. Purified wild-type *Av2* and *Av1* had specific activities of 2500 and 2200 nmol of H_2 (min mg protein)$^{-1}$ at 30 °C, respectively, when assayed in the presence of an optimal amount of the purified complementary component protein as described previously.[19] Protein concentrations were determined by the Lowry method.

The DJ1007 mutant *Av* strain contains a deletion in the *nifE* gene and a polyhistidine tail located near the carboxy-terminus of the α-subunit. DJ1007 cells were grown as described for the wild-type strain but in the presence of 10 mM urea as a fixed-nitrogen source. When the cell density reached 250 Klett units, the culture was concentrated using a Pellicon cell concentrator (Millipore). The cells were resuspended in Burk medium with no added fixed-nitrogen source and allowed to derepress for 3.5 h during which time *nif*-gene expression occurred. After harvesting, crude extracts were prepared by osmotic shock,[20] followed by centrifugation at 98 000 g for 90 min. The apo-MoFe protein (Δ*nifE*:*Av1*) was purified using immobilized metal-affinity chromatography;[21] an additional Q-Sepharose column was utilized to remove a contaminating protein.

Extraction of FeMoco from *Av1*. *Av1* was purified as above through the gel-filtration step, yielding protein with a specific activity of ∼1000 nmol of H_2 (min mg protein)$^{-1}$ and a Mo content of ∼1 g-atom per mol of *Av1*. After dialysis to lower the NaCl concentration, the *Av1* was loaded onto a DE-52 cellulose column that had been washed with 50 mM Tris pH 7.4 buffer containing 2 mM $Na_2S_2O_4$. The bound protein was washed with *N*,*N*-dimethylformamide containing 50 mM 2,2′-bipyridine, 5 mM phosphate buffer pH 8, 2 mM $Na_2S_2O_4$, and water (ca. 5% v/v) until the noncofactor iron was completely eluted. The column was then washed with *N*-methylformamide (NMF) containing 5 mM phosphate buffer pH 8, 2 mM $Na_2S_2O_4$, and water (ca. 5% v/v), and FeMoco was then eluted with NMF that contained 500 mM tetraethylammonium chloride, 5 mM phosphate buffer pH 8, 2 mM $Na_2S_2O_4$, and water (ca. 5% v/v). The eluted FeMoco was concentrated approximately 20-fold by distilling off the NMF under vacuum at 40 °C. FeMoco was assayed[22] by reconstitution of the DJ42 *Av* strain, which has a deletion for the FeMo-cofactor biosynthetic genes *nifENX*. The FeMoco used in this study activated a DJ42 crude extract and produced 75 nmol of H_2 (min mg protein)$^{-1}$.

Nuclear Resonance Vibrational Spectroscopy. For NRVS measurements, samples were loaded into 3 × 7 × 1 mm^3 Lucite cuvettes inside an anaerobic glovebox and frozen. The tops of the cuvettes were sealed with thin Kapton tape to allow better escape of the internal conversion Fe K X-ray fluorescence. ^{57}Fe NRVS spectra were recorded using published procedures[17] at beamline 3-ID at the Advanced Photon Source (APS)[23] and beamline 9-XU at SPring-8.[24] During the measurements, samples were maintained at low temperatures using liquid He. Spectra were recorded between −20 and 80 meV in 0.25 meV steps, using avalanche photodiode detectors.[25] Each scan took ∼40 min. The monochromator energy scales were calibrated using the NRVS of $(NEt_4)(^{57}FeCl_4)$.[26]

Normal Mode Calculations. Spin-unrestricted density functional calculations were carried out using the Jaguar software,[27] the PWPW91 exchange and correlation functional,[28] and the *lacvp** basis set, which combines 6-31G* functions for H, C, N, and O with a double-ζ effective core potential for Fe. All calculations began from the geometry of the cofactor as found in the crystal structure. The homocitrate ligand to Mo was replaced with $(CH_3)_2C(O)CO_2^{2-}$, the histidine with imidazole, and the cysteine ligand to Fe_1 with CH_3S^-; together with a central atom (X = C, N, O, or nothing), this creates the "45-atom" model described earlier.[11] For X = C, N, or O, the formal oxidation states on the metal ions are $Mo^{4+} + 4Fe^{2+} + 3Fe^{3+}$, consistent with Mössbauer and ENDOR assignments and with our earlier calculated redox potentials (see the discussion in ref 11). For X = C, we also investigated a model where one of the bridging sulfides at the "waist" of the cluster was protonated, so that the overall cluster charge was 3−, which we judged to be optimal in earlier redox potential calculations.[11] The model calculations with no central atom used formal metal oxidation states of $Mo^{4+} + 6Fe^{2+} + 1Fe^{3+}$, to have a total cluster charge as close as possible to the other models while maintaining an odd number of electrons. For X = N, the spin alignment we have labeled *bs7*[11,29] was found to be lowest in energy, with the *bs6* state next lowest, and we carried out vibrational calculations on both; for X = C, O, or nothing,

(17) Sturhahn, W. *J. Phys.: Condens. Matter* **2004**, *16*, S497−S530.
(18) Strandberg, G. W.; Wilson, P. W. *Can. J. Microbiol.* **1968**, *14*, 25−31.
(19) Kim, C.-H.; Newton, W. E.; Dean, D. R. *Biochemistry* **1995**, *34*, 2798−2808.
(20) Shah, V. K.; Davis, L. C.; Brill, W. J. *Biochim. Biophys. Acta* **1972**, *256*, 498−511.
(21) Christiansen, J.; Goodwin, P. J.; Lanzillota, W. N.; Seefeldt, L. C.; Dean, D. R. *Biochemistry* **1998**, *37*, 12611−12623.
(22) Paustian, T. D.; Shah, V. K.; Roberts, G. P. *Biochemistry* **1990**, *29*, 3515−3522.
(23) Toellner, T. *Hyperfine Interact.* **2000**, *125*, 3−28.
(24) Yoda, Y.; Yabashi, M.; Izumi, K.; Zhang, X. W.; Kishimoto, S.; Kitao, S.; Seto, M.; Mitsui, T.; Harami, T.; Imai, Y.; Kikuta, S. *Nucl. Instrum. Methods Phys. Res., Sect. A* **2001**, *467*, 715−718.
(25) Kishimoto, S.; Yoda, Y.; Seto, M.; Kitao, S.; Kobayashi, Y.; Haruki, R.; Harami, T. *Nucl. Instrum. Methods Phys. Res., Sect. A* **2004**, *513*, 193−196.
(26) Smith, M. C.; Xiao, Y.; Wang, H.; George, S. J.; Coucovanis, D.; Koutmos, M.; Sturhahn, W.; Alp, E. E.; Zhao, J.; Cramer, S. P. *Inorg. Chem.* **2005**, *44*, 5562−5570.
(27) *Jaguar*, version 6.0; Schrodinger, LLC: New York, 2005.
(28) Perdew, J. P.; Chevary, J. A.; Vosko, S. H.; Jackson, K. A.; Pedersen, M. R.; Singh, D. J.; Fiolhais, C. *Phys. Rev. B* **1991**, *46*, 6671−6687.
(29) Lovell, T.; Li, J.; Liu, T.; Case, D. A.; Noodleman, L. *J. Am. Chem. Soc.* **2001**, *123*, 12392−12410.

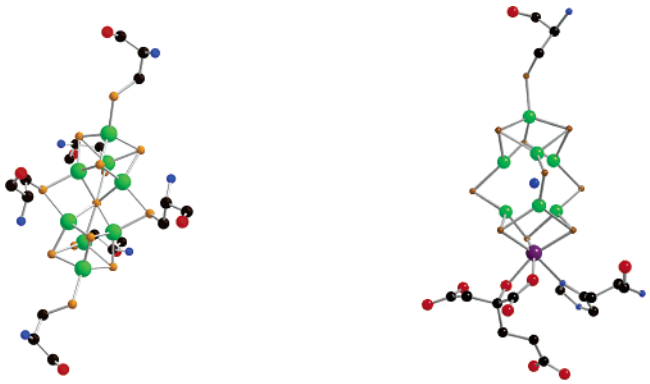

Figure 1. Crystal structure models for (left) P-cluster and (right) FeMo-cofactor.

we used the *bs7* spin alignment. Further details of the calculations will be reported elsewhere. Vibrational densities of states were computed using a Gaussian broadening of 8 cm^{-1}. The empirical normal mode calculations were carried out on FeMo-co models using a Urey−Bradley force field and a special modification of program "Vibratz" to calculate the NRVS spectra.[30]

Results and Discussion

Crystallographic models for the P-cluster and FeMo-cofactor are shown in Figure 1, and the ^{57}Fe PVDOS for ^{57}Fe-enriched *Av1* is shown in Figure 2. This spectrum reflects the overlap of dozens of bands from both FeMo-cofactors and P-clusters, each of which could contribute more than 60 normal modes. To simplify the analysis, we recorded spectra for the Δ*nifE* mutant *Av1* that only contains P-clusters, as well as for isolated FeMoco (Figure 2). The Δ*nifE* mutant sample exhibits an extremely broad spectrum, presumably because the P-clusters have two sets of coupled Fe atoms in three distinct environments. The strongest band (130−160 cm^{-1}) can be assigned to S−Fe−S bending. The only other distinct feature (240−265 cm^{-1}) in the P-cluster spectrum derives from Fe−S stretching motion. Assuming that the P-clusters change little between wild-type and Δ*nifE*:*Av1* proteins, an *Av1* minus Δ*nifE*:*Av1* difference spectrum should reflect just the FeMo-cofactor ^{57}Fe density of states.

The *Av1* minus Δ*nifE*:*Av1* difference spectrum PVDOS (Figure 2) is dominated by a peak near 188 cm^{-1} with a resolved shoulder at 172 cm^{-1}, where there is much less intensity in the Δ*nifE*:*Av1* spectrum. The same pair of features is seen in the isolated FeMoco spectrum, which also has a higher energy band at 208 cm^{-1} (Figure 2). In both the isolated FeMoco and difference spectra, there are S−Fe−S bend modes around 140 cm^{-1}, as well as strong bands related to Fe−S stretching motion at ∼270 and ∼320 cm^{-1}, with additional modes seen out to >400 cm^{-1}. On the low energy side, below ∼100 cm^{-1}, there are features corresponding to cluster torsional modes and larger scale motion of the protein skeleton.

What does the PVDOS tell us about the N_2ase FeMo-cofactor and isolated FeMoco? Empirically, the most striking difference with Fe−S cluster model compounds is the set of strong bands around 190 cm^{-1}. By comparison, a 4Fe model cluster has low NRVS intensity in this region (Figure 2).[31] Modes related to Fe−S−Fe bending motion are between 130 and 160 cm^{-1} in

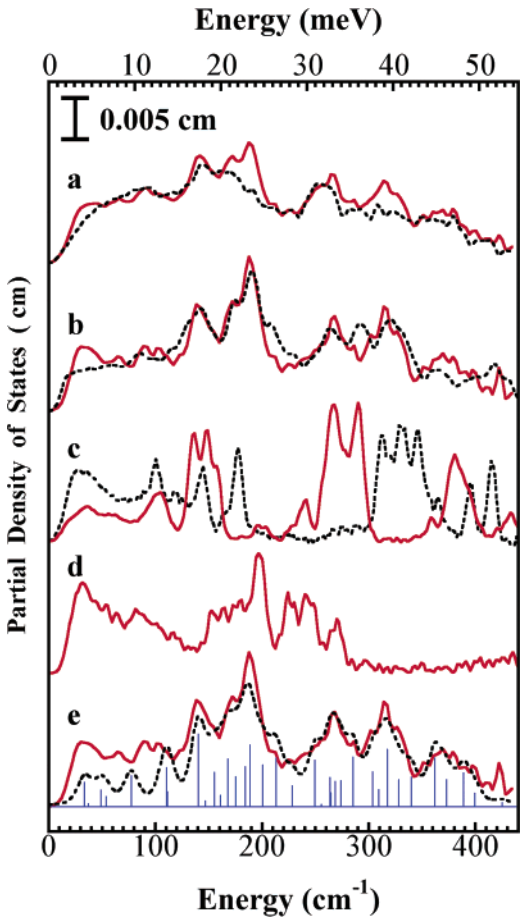

Figure 2. Experimental ^{57}Fe PVDOS functions, $D_{Fe}(\bar{\nu})$, for (top to bottom) (a) *Av1* (—) vs Δ*nifE*:*Av1* (- - -); (b) *Av1*-Δ*nifE*:*Av1* difference spectrum (—) vs isolated FeMoco (- - -); (c) $[Fe_4S_4(SPh)_4]^{2-}$ (—) vs $[Fe_2S_2Cl_2]^{2-}$ (- - -); (d) $[Fe_6N(CO)_{15}]^{3-}$ and (e) *Av1*-Δ*nifE*:*Av1* (—) vs Urey−Bradley simulation (- - -) (sticks represent amplitude of modes before broadening).

Fe_4S_4 clusters.[31] NRVS bands are also observed from 130 to 160 cm^{-1} for the protein-bound FeMo-cofactor and isolated FeMoco but at lower intensity than the 180−190 cm^{-1} features. In diferric Fe_2S_2 clusters, Fe−S−Fe bending modes are at 140−180 cm^{-1} (Figure 2).[26] NRVS spectra are not yet available for Fe_3S_4 clusters, but DFT calculations suggest that their strongest bending modes will also peak around 150 cm^{-1} (Supporting Information). Furthermore, in the models, the strongest PVDOS features are in the Fe−S stretching region above ∼250 cm^{-1}. In summary, the 190 cm^{-1} peak is unusual both in its position and in its relative NRVS intensity.

One Fe cluster that does have significant intensity in modes near 190 cm^{-1} is $[Fe_6N(CO)_{15}]^{3-}$ (Figure 2). This quasi-octahedral CO-bridged complex has limitations as a model for the trigonal prismatic FeMo-cofactor cluster; nevertheless, it appears relevant that the strongest peak in its spectrum is a breathing mode for the Fe_6 octahedron at 195 cm^{-1}. By comparison, breathing modes for $[Fe_4S_4(SR)_4]^{2-}$ cubane models occur near 145 cm^{-1}.[31] We attribute the higher frequency in $[Fe_6N(CO)_{15}]^{3-}$ and the FeMo-cofactor/FeMoco in part to the extra rigidity conferred by bonding to an interstitial atom.

One approach to interpretation of vibrational spectra is the use of empirical potentials. In the past, Urey−Bradley force fields (UBFF) have successfully been applied to mononuclear Fe sites in rubredoxins,[32] 2Fe[33,34] and 4Fe ferredoxins and model complexes,[35] and, more recently, $MoFe_3S_4$ clusters.[36,37] For our

(30) Dowty, E. *Phys. Chem. Miner.* **1987**, *14*, 67−79.
(31) Xiao, Y.; Koutmos, M.; Case, D. A.; Coucouvanis, D.; Wang, H.; Cramer, S. P. *J. Chem. Soc., Dalton Trans.* **2006**, 2192−2201.

Table 1. Force Constants Used for Normal Mode Simulations on *Av1* − Δ*nifE*:*Av1* Difference Spectrum using $[O_3MoFe_7NS_9(SC)]^{n-}$ Model and Intact FeMo-cofactor with Crystallographic Coordinates

K (mdyne/Å)		H (mdyne–Å/rad²)		F (mdyne/Å)	
Fe−$S^{\mu 2}$	1.03	$S^{\mu 3}$−Fe−$S^{\mu 3}$	0.0	O···O	0.07
	1.44[b]	$S^{\mu 3}$−Fe−$S^{\mu 2}$			
Fe−$S^{\mu 3}$	0.74	S−Fe−N	0.36	S···O	0.12
	0.8, 0.95				
	0.98, 1.06[c]				
Fe^t−$S^{\mu 3}$	1.16	Fe−N−Fe	0.44	$S^{\mu 3}$···$S^{\mu 3}$	0.14
	1.44[b]				
Fe^t−S^{cys}	1.34	S−Mo−S	0.35	$S^{\mu 3}$···N	0.21
	1.12				
	1.36[d]				
Fe−N	0.32	O−Mo−O	0.53	$S^{\mu 3}$··· $S^{\mu 2}$	0.03
Mo−S	2.05	S−Mo−O	0.34	$S^{\mu 2}$···N	0.08
	2.13[d]				
Mo−O	2.1	Fe−$S^{\mu 3}$−Fe	0.3	$S^{\mu 3}$···S^{cys}	0.08
	2.06[d]				
Fe−Fe	0.27	Fe−S−Mo	0.61		
Mo−Fe	0.35	Fe^t−S^{cys}−C	0.21		
S^{cys}−C	3.24				

[a] $S^{\mu 2}$: doubly bridging S. $S^{\mu 3}$: triply bridging S. S^{cys}: cysteine S. Fe^t: terminal Fe. [b] Reference 26. [c] Reference 36. [d] Reference 37.

analysis, we built (in silico) a 23-atom model with C_{3v} symmetry. The Mo end of the cluster was terminated with three oxygens, whereas an S−C ligand was used at the Fe end (Figure 5). We then optimized the UBFF parameters so that the $16A_1$, $5A_2$, and 21 doubly degenerate E normal modes best simulated the experimental *Av1* − Δ*nifE*:*Av1* PVDOS.

What structural features and parameters give rise to the unusual FeMo-cofactor spectrum? As summarized in Table 1, the Fe−S force constants that we arrived at are similar to or lower than those used by other groups to model Fe_4S_4 clusters,[35,36] and the Fe−Fe interaction constant is also not unusual, 0.27 mdyne/Å compared to 0.19[35] or 0.22−0.36 mdyne/Å.[37] By themselves, none of the parameters would drastically alter the spectrum. One special feature of the model is of course the "interstitial" atom. Assuming a central N, the UBFF simulations are optimized with Fe−N stretching force constants of ∼0.3 mdyne/Å. With this force field, several strong Fe breathing modes appear between 170 and 210 cm^{-1} (Figure 5). Because the central atom contributes little to the kinetic energy of these low-frequency modes, similar conclusions would be reached with the same force constants for interstitial C or O.

As noted by Lee and Holm,[38,39] there are no really good models for N bound to weak-field Fe in an FeMo-cofactor-like geometry. (However, there has been some recent progress in this area[40]). In μ-nitrido bridged low-spin Fe(III) porphyrin dimers, Fe−N force constants as high as 4.5 mdyne/Å have been reported,[41] compared to a 2.2 mdyne/Å value reported for

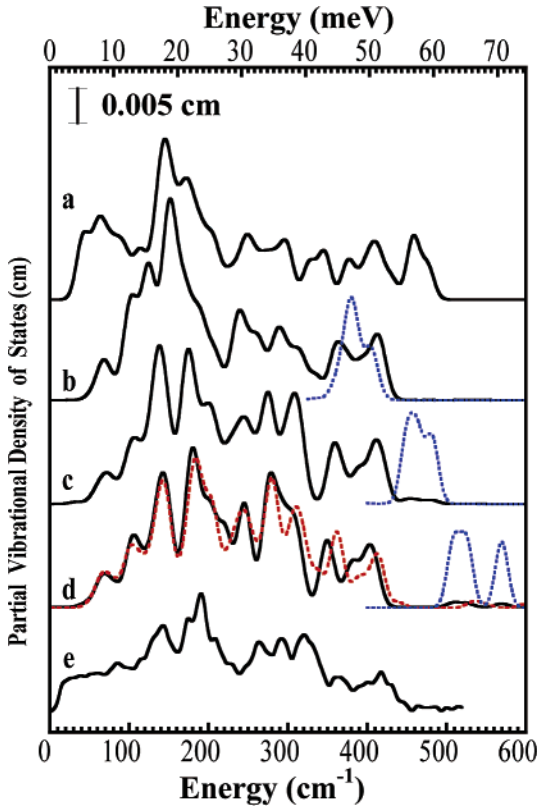

Figure 3. DFT-calculated ^{57}Fe (—) and light atom (· · ·) PVDOS for (top to bottom) (a) empty site; (b) "X=O^{2-}"; (c) "X=N^{3-}"; (d) "X=C^{4-}" vs "X=C^{4-}, H^+" (- - -) (light atom not shown); (e) isolated FeMoco spectrum.

hexacoordinate N in $[Fe_6N(CO)_{15}]^{3-}$.[42] Assuming an Fe−N distance of ∼2.05 Å, a Badger's rule calculation for K (Fe−N) yields ∼0.49 mdyne/Å. Thus, the ∼0.3 mdyne/Å value derived from the simulations indicates a rather weak interaction between the interstitial atom and its neighboring Fe atoms.

Another approach to interpretation of NRVS spectra is first principles calculation of the normal modes using density functional theory (DFT). A set of such calculations for X=O^{2-}, N^{3-}, or C^{4-} is shown in Figure 3. (Of course, in these calculations the final charge on the interstitial atom is much less negative than the formal oxidation state.) For X=O^{2-}, the strongest peak in the calculated PVDOS is at ∼152 cm^{-1}; the maximum shifts to 174 cm^{-1} for X=N^{3-} and to 181 cm^{-1} for X=C^{4-}. Taking the interstitial atom out yields a main peak below 150 cm^{-1} and a flatter intensity distribution between 200 and 500 cm^{-1}.

Although the interstitial C model gives the closest match to the observed PVDOS, it also confers a relatively large negative charge on the cluster. We thus performed a final calculation allowing for protonation of the FeMo-cofactor. This "X = C^{4-}, H^+" model also gave a good simulation of the experimental PVDOS, with a primary peak at 184 cm^{-1}, and generally higher frequencies for most modes (Figures 3 and 4). At the current level of uncertainty between experiment and calculation, none of these models can be absolutely excluded.

Another aid to interpretation of the DFT results is to compare the PVDOS for different atoms within the FeMo-cofactor, as

(32) Czernuszewicz, R. S.; Kilpatrick, L. K.; Koch, S. A.; Spiro, T. G. *J. Am. Chem. Soc.* **1994**, *116*, 1134−1141.
(33) Han, S.; Czernuszewicz, R. S.; Kimura, T.; Adams, M. W. W.; Spiro, T. G. *J. Am. Chem. Soc.* **1989**, *111*, 3505−3511.
(34) Mitou, G.; Higgins, C.; Wittung-Stafshede, P.; Conover, R. C.; Smith, A. D.; Johnson, M. K.; Gaillard, J.; Stubna, A.; Münck, E.; Meyer, J. *Biochemistry* **2003**, *42*, 1354−1364.
(35) Czernuszewicz, R. S.; Macor, K. A.; Johnson, M. K.; Gewirth, A.; Spiro, T. G. *J. Am. Chem. Soc.* **1987**, *109*, 7178−7187.
(36) Kern, A.; Nather, C.; Studt, F.; Tuczek, F. *Inorg. Chem.* **2004**, *43*, 5003−5010.
(37) Kern, A.; Näther, C.; Tuczek, F. *Inorg. Chem.* **2004**, *43*, 5011−5020.
(38) Lee, S. C.; Holm, R. H. *Proc. Natl. Acad. Sci. U.S.A.* **2003**, *100*, 3595−3600.
(39) Lee, S. C.; Holm, R. H. *Chem. Rev.* **2004**, *104*, 1135−1158.
(40) Bennett, M. V.; Stoian, S.; Bominaar, E. L.; Münck, E.; Holm, R. H. *J. Am. Chem. Soc.* **2005**, *127*, 12378−12386.
(41) Crisanti, M. A.; Spiro, T. G.; English, D. R.; Hendrickson, D. N.; Suslick, K. S. *Inorg. Chem.* **1984**, *23*, 3897−3901.
(42) Della Pergola, R.; Bandini, C.; Demartin, F.; Diana, E.; Garlaschelli, L.; Stanghellini, P. L.; Zanello, P. *J. Chem. Soc., Dalton Trans.* **1996**, 747−754.

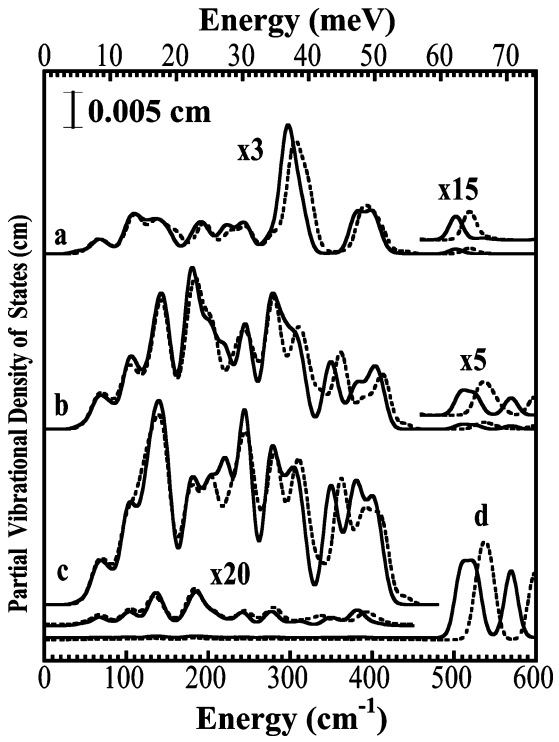

Figure 4. Decomposition of "X=C^{4-}" DFT (—) and "X=C^{4-}, H^{+}" DFT (- - -) into (top to bottom) (a) Mo, (b) Fe, (c) S, and (d) C PVDOS.

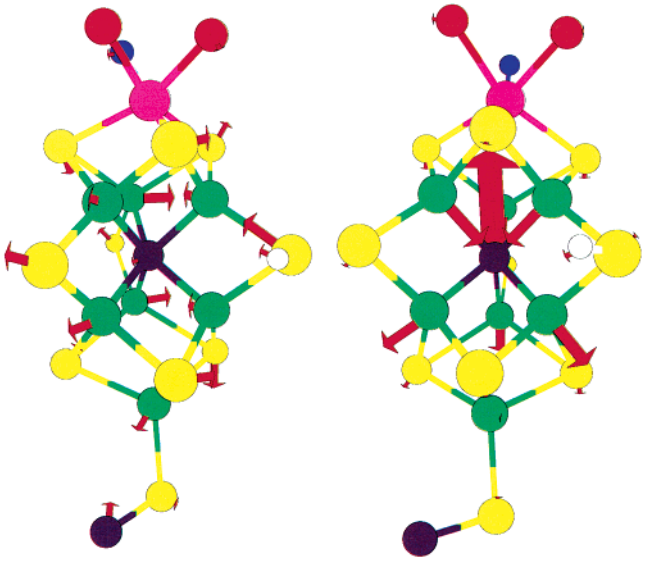

Figure 5. Simplified FeMo-cofactor model with arrows indicating relative atomic motion as calculated from DFT theory for (left) a breathing mode at 177 cm^{-1} and (right) a "shake" mode at 599 cm^{-1}. Color scheme is as follows: Fe, green; Mo, purple; S, orange; C, black; N, blue; and O, red.

we have done for Fe and the interstitial X in Figure 3 and for Mo, Fe, S, and interstitial C in Figure 4. We have also illustrated the relative motions for two key predicted modes of the "X=C^{4-}, H^{+}" model in Figure 5. As expected, the breathing modes with strong NRVS intensity have little interstitial atom motion and, hence, are very insensitive to light atom isotopic substitution. In contrast, we see that the interstitial has the greatest amount of motion in modes ranging from 350 to 420 cm^{-1} (X=O^{2-}) through 430−500 cm^{-1} (X=N^{3-}) to 480−590 cm^{-1} (X=C^{4-}). These modes are all quite sensitive to the mass of the light atom. The Fe—S stretch modes between 220 and 420 cm^{-1} involve substantial S motion and, hence, will exhibit measurable $^{32}S/^{36}S$ isotope shifts. With both DFT and UBFF, the atomic motions for the strongest NRVS modes can be described as breathing and/or bending of the central Fe cage. Some of the frequency differences arise from changes in the stiffness of these motions depending on the presence and nature of the interstitial atom.

The interstitial X "shake" modes, shown in Figure 5, have been discussed extensively in the context of $[M_6X(CO)_x]^{n-}$ clusters,[42,43] but they have yet to be observed for N_2ase or FeMo-co. In the DFT calculations, the "shake" modes for the FeMo-cofactor with X=N (430−500 cm^{-1}) or C (480−590 cm^{-1}) are predicted to have much lower frequencies than the corresponding modes that are actually observed centered around 765 or 790 cm^{-1} in $[Fe_6N(CO)_{15}]^{3-}$ or $[Fe_6C(CO)_{16}]^{2-}$, respectively;[42−44] this is consistent with a larger cavity in the FeMo-cofactor (e.g., mean Fe−X distance of 2.00 Å vs 1.86 Å in $[Fe_6N(CO)_{15}]^{3-}$). Since they primarily involve oscillation of X, either along or perpendicular to the cluster approximate symmetry axes, there is little Fe motion in the "shake" modes and hence a very small predicted NRVS signal. With approximate *ungerade* symmetry, they are also very weak in Raman spectroscopy. However, the motion of the charged interstitial gives rise to a large transition dipole, and these modes have strong infrared signals and large light atom isotope shifts. Attempts to exploit these predictions are of course underway.

In summary, the vibrational spectra derived from NRVS experiments support the presence of an interstitial atom in both isolated FeMoco and in the *Av1*-bound FeMo-cofactor. Future experiments by NRVS and other vibrational spectroscopies over a wider range of frequencies should help identify the chemical nature of the interstitial atom and help elucidate changes that occur during the catalytic mechanism of this enzyme.

Acknowledgment. This work was funded by NIH grants GM-44380 (S.P.C.), GM-65440 (S.P.C.), GM-39914 (D.A.C.), and DK-37255 (W.E.N.) and the DOE Office of Biological and Environmental Research (S.P.C.). Use of the Advanced Photon Source is supported by the U.S. Department of Energy, Basic Energy Sciences; Office of Science, under Contract No. W-31-1-9-Eng-38. SPring-8 is supported by JASRI.

Supporting Information Available: Potential Energy Distribution (PED) of representative normal modes in NRVS from normal-mode analysis for FeMo-cofactor in nitrogenase is summarized in Table S1. A PVDOS comparison between $[Fe_3S_4(SCH_3)_3]^{3-}$ and FeMo-cofactor using DFT calculation is shown in Figure S1. This material is available free of charge via the Internet at http://pubs.acs.org.

JA0603655

(43) Creighton, J. A.; Dellapergola, R.; Heaton, B. T.; Martinengo, S.; Strona, L.; Willis, D. A. *J. Chem. Soc., Chem. Commun.* **1982**, 864−865.
(44) Stanghellini, P. L.; Rossetti, R. *Comments Inorg. Chem.* **1990**, *9*, 263−303.